

The numerical analysis of a vertical axis turbine for current energy conversion

Min-Hsiung Yang^{#1}, Zih-Duan Ciou^{#2}, Syue-Sinn Leu^{#3}, Jun-Lum Cai^{#4}, Wei-Ren Chau^{#5}

[#] Department of Naval Architecture and Ocean Engineering, National Kaohsiung Marine University

¹ mhyang@webmail.nkmu.edu.tw

² 1051535111@stu.nkmu.edu.tw

³ ssleu@webmail.nkmu.edu.tw

Abstract—The ocean current energy is plentiful on the coastline of Taiwan. The conversion effect of a current turbine is the important issue in application. The purpose of this study is to analyze the performance of a vertical axis turbine consisting of deflectable blades applied in ocean current energy conversion. The detailed flow field analyses and the characteristics of the turbine are investigated numerically. Finally, the performance and optimal prediction of the turbine are obtained.

The variable blades could increase the torque and decrease the resistance of the vertical axis turbine. The commercial code ANSYS-Fluent CFD is employed to simulate and calculate the performance of the novel vertical axis turbine. The results of the velocity contours of calculation domain are reported. Furthermore, the torque and power coefficient of the vertical axis turbine at various rotation angle are obtained. The maximum power coefficient and the corresponding optimal tip speed ratio are also reported numerically.

Keywords—Current energy, Ocean, Vertical axis turbine, Drag type, Performance.

Nomenclature

B	breadth of the blade, m
C_p	power coefficient
H	height, m
P_{out}	power, W
Q	torque, N-m
V_0	averaged velocity, m/s

Greek symbols

α	deflection angle of blade, °
θ	rotation angle of entire DBT, °
ρ	density, kg/m ³
ω	angular velocity of the DBT, rad/s

Acronyms

TSR	tip speed ratio
-------	-----------------

I. INTRODUCTION

Energy shortage and environmental protection have become important issues for energy utilization. Ocean current and tidal energy are renewable, predictable and continual. The vertical axis turbine (VAT) driven by multi-directional current flow

has been widely applied in current energy conversion [1]. Many researchers have adopted various techniques to improve the performance for the vertical axis turbine. [2-3]. Moreover, numerical and experimental analyses of vertical axis turbines with drag blades were reported [4-6]. The Savonius turbine is a drag type of vertical axis tidal turbine with great development potential. The rotating motion of Savonius turbine is based on the drag coefficient of a concave surface larger than that of the convex surface [7-8]. Modified Savonius turbines with deflector plate have been proposed [9-11] to increase the power output or enhance the efficiency for current energy applications. This paper is to investigate the performance of a vertical axis turbine (VAT) applied in ocean current and tide energy conversion. The detailed flow field analyses and the VAT characteristics are investigated numerically.

II. ANALYSIS OF THE VAT

The vertical axis turbine consists of five drag type blades and one set of cam device for current energy conversion, as shown in Fig. 1. Each blade not only rotates around the centre of entire turbine, but also enables to deflect around its deflecting axis, individually.

The deflecting actions of the blade are achieved by the mechanism of the cam device. As the cam nose pushes the concave surface of advancing blade, this blade will deflect to enlarge the effective area of concave surface and generate a higher drag force downstream. Meanwhile, the other blades, which are affected by the current, shrinks and reduces the effective area of convex surface to decline the reversing resistance upstream, as shown in Fig. 2. Therefore, the net generating torque of whole turbine can be enlarged and could produce higher net power output.

The rotation angle, θ of the VAT and the deflection angle, γ of blade are depicted in Fig. 3. Furthermore, the relationship of rotation angle and the deflection angle of the VAT are demonstrated clearly in Fig. 4. As θ increase from -72° to 0° , the blade open rapidly and the deflection angle increase from

0° to 180°. The relationship of the variations for the rotation angle and the deflection angle can be conducted as:

$$\Delta\theta = 2.5 \Delta\gamma \quad (1)$$

In addition, from $\theta=0^\circ$ to 72° , the blade close gradually, and the deflection angle decrease from 180° to 108° . Furthermore, the relationship of θ and γ can be expressed as

$$\Delta\theta = -\Delta\gamma \quad (2)$$

Moreover, the blade keeps closed as the VAT rotates from $\theta=72^\circ$ to -72° . The geometric parameters of the VAT for this study are demonstrated in Fig. 5 and the values of these parameters are listed in Table 1.

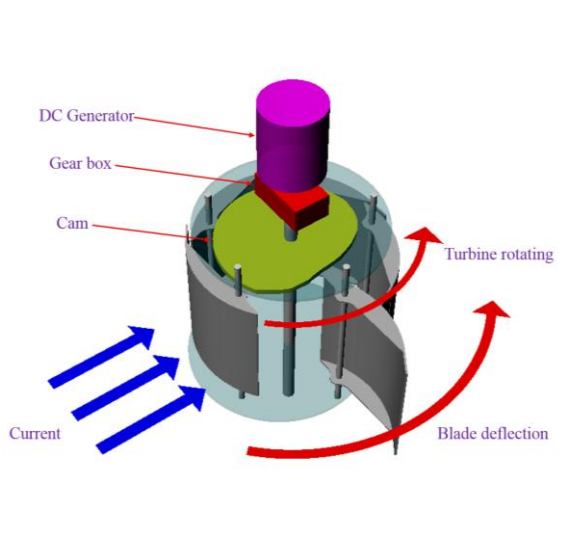


Fig. 1 The vertical axis turbine consisting of deflectable blades

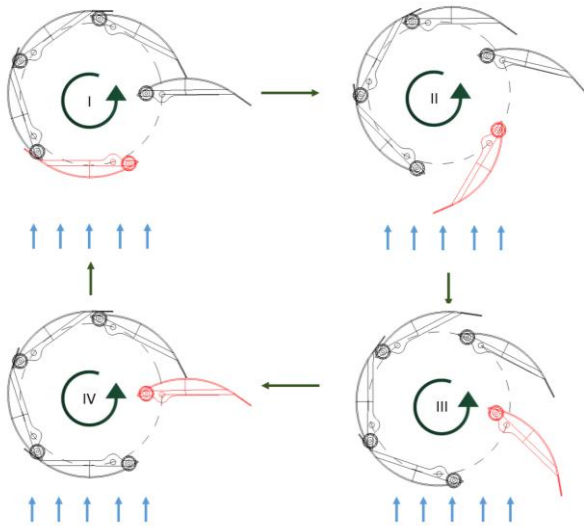


Fig. 2 The deflections of blade various position

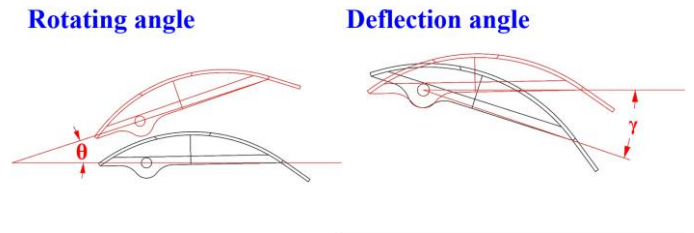


Fig. 3. The rotating angle and deflectable angle.

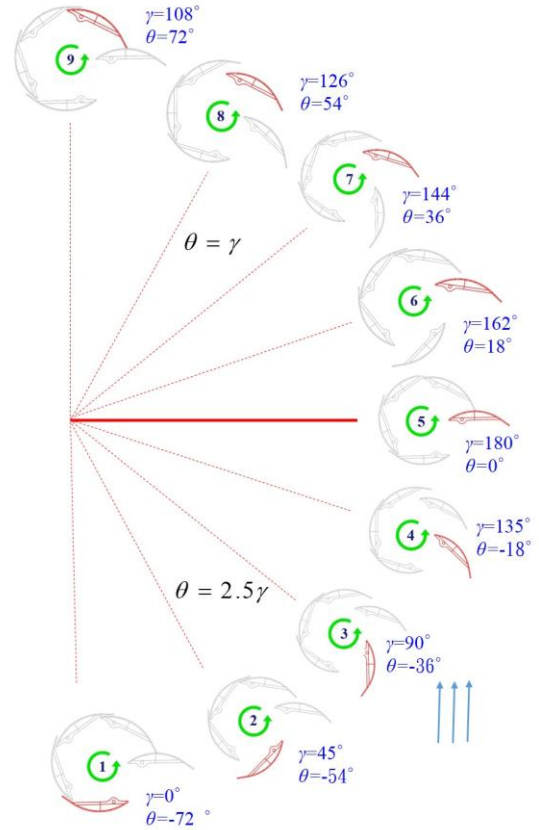


Fig. 4. The relationships of blade deflection and rotation

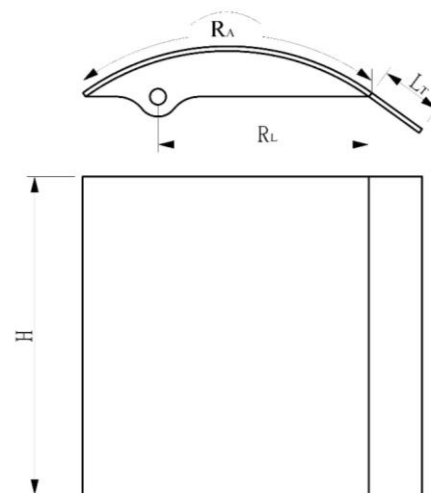


Fig. 5. The definition of the geometric parameters.

Table 1. The geometric parameters of VAT

Parameter	Description	Value	Unit
B	Breadth of blade	0.200	m
H	Height	0.3	m
L_L	Long connecting rod	0.183	m
L_S	Short connecting rod	0.142	m
R_C	Rotating radiuses of DBT	0.151	m
R_L	Deflecting radiuses of blades	0.1	m
R_R	Rotating radiuses of the ring	0.05	m
θ	Rotation angle of the DBT	$0^\circ \sim 360^\circ$	
γ	Deflection angle of blade	$0^\circ \sim 180^\circ$	

III. PERFORMANCE ANALYSIS

The net force of one blade can be evaluated by integrating the pressure difference between concave surface and convex surface areas. Furthermore, the torque generated by one blade can be calculated from the net force multiplying the distance between the rotation centre of the VAT and the deflection centre of the blade. Furthermore, the total torques, Q_{tot} of the VAT is summed by the torque of each blade. Therefore, the power output of VAT can be written as

$$P_{out} = Q_{tot} \times \omega \quad (3)$$

where, ω is the angular velocity of VAT. Furthermore, to investigate the effect of angular velocity on the performance of VAT, a dimensionless parameter, tip speed ratio (TSR), is defined as

$$TSR = \frac{\omega(R_C / 2 + R_L)}{V_0} \quad (4)$$

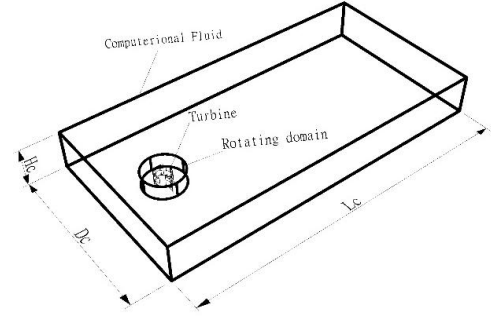
Likewise, to evaluate the performance of current-energy-conversion efficiency, a dimensionless power coefficient, C_p , of the VAT is defined as

$$C_p = \frac{P_{out}}{\frac{1}{2} \rho [(2R_C + R_L) \times H] V_0^3} \quad (5)$$

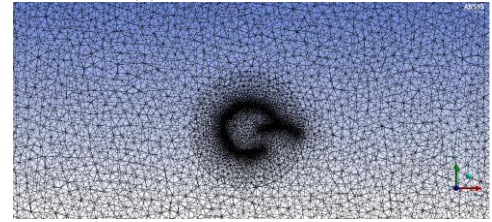
A commercial code of Ansys Fluent based on finite volume method is employed for 3-D simulation in this study. The computational domain of this study is showed in Fig. 6 (a). The outlet boundary condition is assumed as zero gauge (atmospheric) pressure. The boundaries of walls are no-slip conditions. The standard $k-\omega$ turbulence model is applied in these calculations. The pressure-velocity coupling of momentum equations are solved by using the SIMPLE-C scheme. The rotation flow region is discretized using a finer mesh, whereas the main flow region uses a coarser mesh as shown in Fig. 6(b). The variations of total torques of the VAT, Q_i with various elements at $V_0=1$ m/s, $\omega=1.885$ rad/s, $\gamma=0$ and $\theta=-72^\circ$ are depicted in Fig. 6(c).

In grid independent examination, the last five sets give the same results, substantially. Finally, the total grid number is

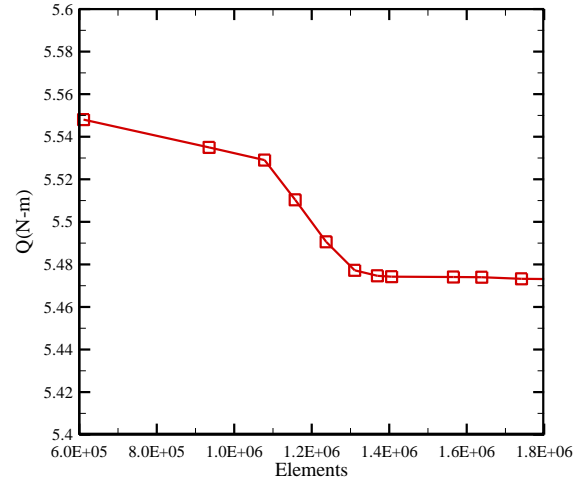
larger than 1,360,000 used in this study for simulation. To simplify the simulation of the VAT, the influences of the accessories are neglected in this study.



(a)



(b)



(c)

Figs. 6 (a) The entire computational domains, (b) the grid distributions near VAT, and (c) the grid independent examination.

Furthermore, in this section, the velocity of stream is assumed of $V_0=1$ m/s. To depict the visual results of simulations concisely, only 4 rotation angles, $\theta=-63^\circ$, -54° , -45° , -36° , -27° , -18° , -9° and 0° of Blade 1 are selected and revealed. The streamlines, velocity contours, and torque distribution are analysed and discussed as the current flows through the VAT. Figure 7 displays the 3-D flow streamlines near the VAT with various rotating positions at $\omega=1.885$ rad/s.

Then, the velocity contours from top view for the VAT for various rotating positions are demonstrated in Fig. 8. Finally, torque distribution of each blade for various rotation angles are revealed in Fig. 9.

At $\theta=-63^\circ$, it is obvious in Fig. 7 that as the streamlines pass through the Blade 1, smoothly. As rotation angle, θ , increases to -36° , the Blade 1 opens gradually, and those large eddies near the convex surface of Blade 1 also increase progressively. Subsequently, as the VAT rotates to 0° , the deceleration zones behind Blades 1 become more evident, and a large vortex emerges in downstream region.

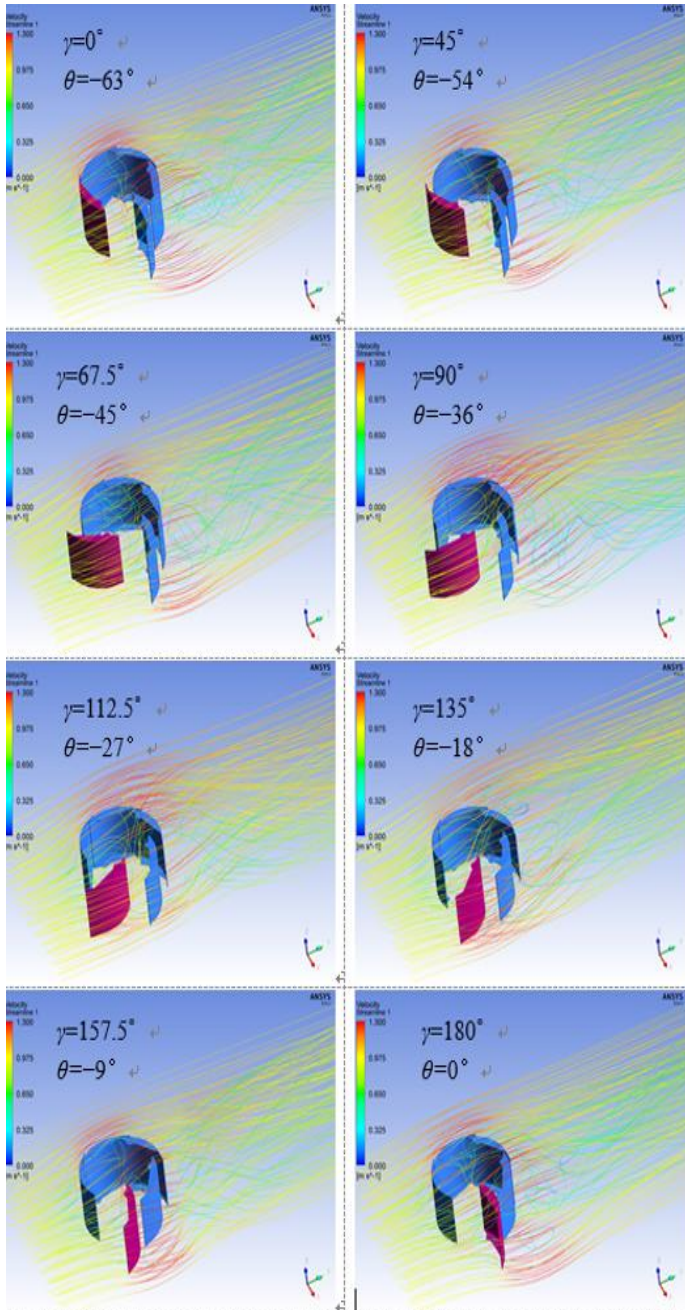


Fig. 7. The streamline distributions of VAT at $V_0=1$ m/s and $\omega=1.885$ rad/s.

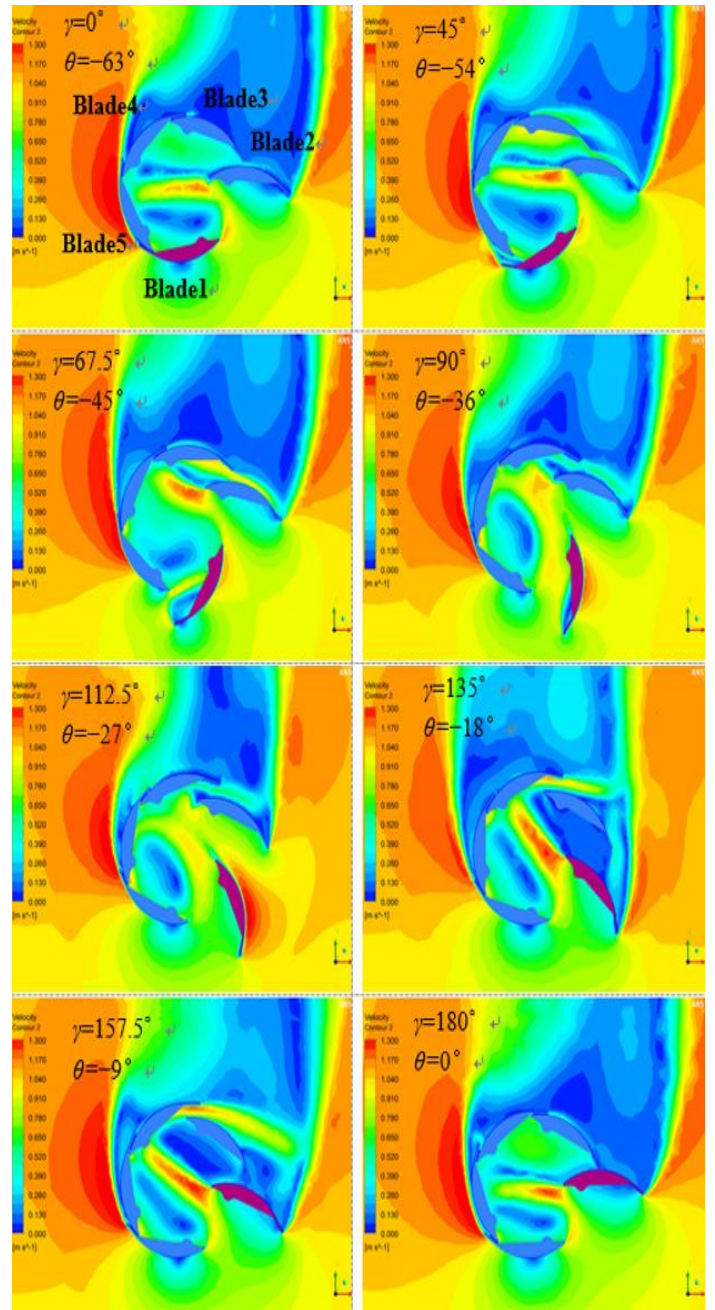


Fig. 8. The velocity contours for various rotating position of VAT at $V_0=1$ m/s and $\omega=1.885$ rad/s.

At $\theta=-63^\circ$, the Blade 2 locates downstream and takes over the most significant responsibility to produce torque, as shown in Fig. 9. Meanwhile, it should be noted that Blade 1 contributes negative torque since it rotates at upstream flow and deflects to oppose the current flow. As rotation angle, θ increases to -36° , the torque output of the Blade 1 increases. At $-27^\circ < \theta < 0^\circ$, the Blade 1 pushed by the current and plays the most important role for generating torque. Note that the maximal torque output of the Blade 1 occurs at $\theta=-18^\circ$.

At $0^\circ < \theta < 27^\circ$, the Blade 1 also generates higher positive torque. As θ increases from 27° to 54° , the torque decrease obviously. The total torque generated by these blades of the

VAT is also demonstrated with various rotation angles. It can be observed that as θ increase from -72° to -45° , the total torque, Q_{SUM} remain in lower values. Furthermore, the total torque increase obviously at $-45^\circ < \theta < -27^\circ$. The VAT performs higher total torque at $-27^\circ < \theta < -18^\circ$. Then the Q_{SUM} decreases with rotation angle at $-18^\circ < \theta < 0^\circ$.

The VAT is designed for the floating type of vertical axis turbine in real application. Figure 10 demonstrates the variations of power coefficient, C_p with various TSR of the VAT. It is clear that a concave downward curve of the C_p can be observed $V=1$ m/s. Moreover, the value of maximal power coefficient, $C_{p,max}$ and its corresponding optimal tip speed ratio, TSR_{opt} also can be obtained for VAT.

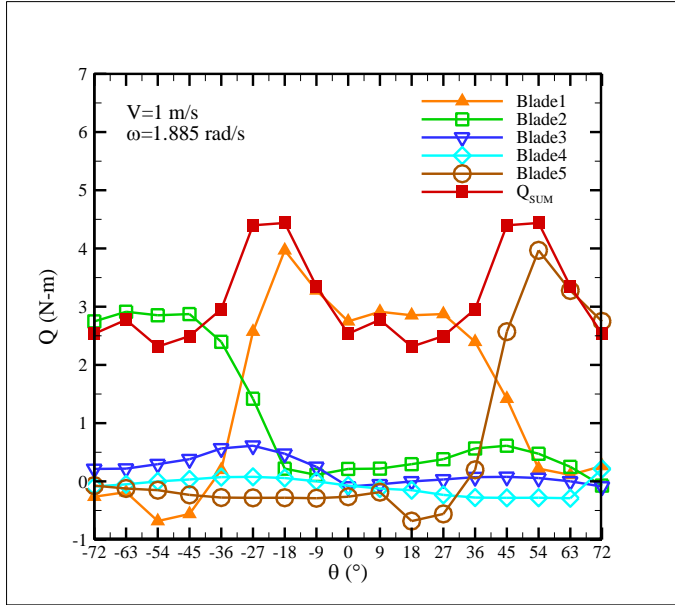


Fig. 9. Torque distribution of each blade with various rotating positions.

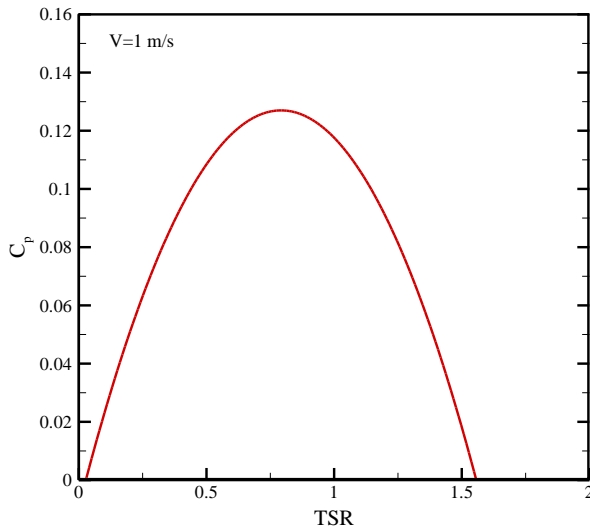


Fig. 10. The variation of C_p with various TSR .

IV. CONCLUSIONS

An analysis of a vertical axis turbine which consists of deflectable blades is conducted to improve the efficiency of ocean current energy conversion. Numerical investigations of the VAT are presented. The optimal predictions of VAT are depicted as ocean current velocity is 1m/s. The results support the conclusions below:

1. The motions of VAT are investigated numerically. Moreover, the streamlines, velocity contours of the current flow near the VAT at $V_0=1$ m/s are analysed.
2. The torque generated by each blade of the VAT with various rotation angles is obtained numerically. The maximum and minimum of total torque for VAT occurs at $\theta=-18^\circ$ and $\theta=-54^\circ$, respectively at $V_0=1$ m/s.
3. The Blade 1 plays the most important role for generating torque at $-27^\circ < \theta < 27^\circ$.

ACKNOWLEDGMENT

The financial support for this research from the Engineering Division of the Ministry of Science and Technology, Republic of China, through contract 106-2628-E-022 -001 -MY3, is greatly appreciated.

REFERENCES

- [1] Chen L, Lam W. A review of survivability and remedial actions of tidal current turbines. *Renewable and Sustainable Energy Reviews* 2015;43:891-900.
- [2] Hwang IS, Lee YH, Kim SJ. Optimization of cycloidal water turbine and the performance improvement by individual blade control. *Applied Energy* 2009;86:1532-40.
- [3] Yang B, Lawn C. Fluid dynamic performance of a vertical axis turbine for tidal currents. *Renewable Energy* 2011;36:3355-66.
- [4] Rolland SA, Thatcher M, Newton W, Williams AJ, Croft TN, Gethin DT et al. Benchmark experiments for simulations of a vertical axis wind turbine. *Applied Energy* 2013;111:1183-94.
- [5] Rolland S, Newton W, Williams AJ, Croft TN, Gethin DT, Cross M. Simulations technique for the design of a vertical axis wind turbine device with experimental validation. *Applied Energy* 2013;111:1195-203.
- [6] Li Y, Calisal SM. Three-dimensional effects and arm effects on modeling a vertical axis tidal current turbine. *Renewable Energy* 2010;35:2325-34.
- [7] Roy S, Saha UK. Wind tunnel experiments of a newly developed two-bladed Savonius-style wind turbine. *Applied Energy* 2015;137:117-25.
- [8] Golecha K, Eldho TI, Prabhu SV. Influence of the deflector plate on the performance of modified Savonius water turbine. *Applied Energy* 2011;88:3207-17.
- [9] Ricci R, Romagnoli R, Montelpare S, Vitali D. Experimental study on a Savonius wind rotor for street lighting systems. *Applied Energy* 2016;161:143-52.
- [10] Shigetomi A, Murai Y, Tasaka Y, Takeda Y. Interactive flow field around two Savonius turbines. *Renewable Energy* 2011;36:536-45.
- [11] Yang MH, Huang GM, Yeh RH. Performance investigation of an innovative vertical axis turbine consisting of deflectable blades. *Applied Energy* 2016;179:875-87.